

# General Invertible Transformations for Flow-based Generative Modeling

**Jakub M. Tomczak**

*Vrije Universiteit Amsterdam*

*the Netherlands*

JMK.TOMCZAK@GMAIL.COM

## Abstract

In this paper, we present a new class of invertible transformations. We indicate that many well-known invertible transformations in reversible logic and reversible neural networks could be derived from our proposition. Next, we propose two new coupling layers that are important building blocks of flow-based generative models. In the preliminary experiments on toy digit data, we present how these new coupling layers could be used in Integer Discrete Flows (IDF), and that they achieve better results than standard coupling layers used in IDF and RealNVP.

**Keywords:** Invertible Neural Networks, Deep Generative Modeling, Normalizing Flows

## 1. Introduction

**Notation** Let us consider a  $D$ -dimensional space  $\mathbf{x} \in \mathcal{X}$ , e.g.,  $\mathcal{X} = \{0, 1\}^D$ ,  $\mathcal{X} = \mathbb{Z}^D$  or  $\mathcal{X} = \mathbb{R}^D$ . We define a binary invertible operator  $\circ : \mathcal{X} \times \mathcal{X} \rightarrow \mathcal{X}$ . The inverse operation to  $\circ$  is denoted by  $\bullet$ . For instance, for the addition:  $\circ \equiv +$  and  $\bullet \equiv -$ , and for the XOR operator:  $\circ \equiv \oplus$  and  $\bullet \equiv \ominus$ . Further, we use the following notation:

- $\mathcal{X}_{i:j}$  is a subset of  $\mathcal{X}$  corresponding to variables from the  $i$ -th dimension to the  $j$ -th dimension,  $\mathbf{x}_{i:j}$ .
- We assume that  $\mathcal{X}_{1:0} = \emptyset$  and  $\mathcal{X}_{n+1:n} = \emptyset$ .

**Invertible transformations** In reversible computing (Toffoli, 1980; Fredkin and Toffoli, 1982), invertible logic gates allow to invert logic operations in order to potentially decrease energy consumption of computation (Bennett, 2003). The typical invertible logic gates are:

- the Feynman gate: For  $\mathbf{x} \in \{0, 1\}^2$ , the gate is defined as follows (Feynman, 1986):

$$\begin{aligned} y_1 &= x_1 \\ y_2 &= x_1 \oplus x_2. \end{aligned} \tag{1}$$

- the Toffoli gate: For  $\mathbf{x} \in \{0, 1\}^3$ , the gate is defined as follows (Toffoli, 1980):

$$\begin{aligned} y_1 &= x_1 \\ y_2 &= x_2 \\ y_3 &= x_3 \oplus (x_1 \wedge x_2). \end{aligned} \tag{2}$$

- the Fredkin gate: For  $\mathbf{x} \in \{0, 1\}^3$ , the gate is defined as follows (Fredkin and Toffoli, 1982):

$$\begin{aligned} y_1 &= x_1 \\ y_2 &= x_2 \oplus (x_1 \wedge (x_2 \oplus x_3)) \\ y_3 &= x_3 \oplus (x_1 \wedge (x_2 \oplus x_3)). \end{aligned} \tag{3}$$

Invertible transformations play also a crucial role in reversible neural networks (Gomez et al., 2017; Chang et al., 2018; MacKay et al., 2018). For instance, an invertible transformation called a *coupling layer* is an important building block in flow-based models (Dinh et al., 2016). It is defined as follows:

$$\begin{aligned} \mathbf{y}_1 &= \mathbf{x}_1 \\ \mathbf{y}_2 &= \exp\{\text{NN}_s(\mathbf{x}_1)\} \odot x_2 + \text{NN}_t(\mathbf{x}_1), \end{aligned} \tag{4}$$

where  $\odot$  is an element-wise multiplication,  $\text{NN}_s(\cdot)$  and  $\text{NN}_t(\cdot)$  denote arbitrary neural networks, and an input is divided into two parts,  $\mathbf{x} = [\mathbf{x}_1, \mathbf{x}_2]$ , e.g., along the channel dimension. If  $\text{NN}_s(\cdot) \equiv 1$ , and we stack two coupling layers with reversing the order of variables in between, then we obtain the reversible residual block (Gomez et al., 2017):

$$\begin{aligned} \mathbf{y}_1 &= \mathbf{x}_1 + \text{NN}_{t,1}(\mathbf{x}_2) \\ \mathbf{y}_2 &= \mathbf{x}_2 + \text{NN}_{t,2}(\mathbf{y}_1). \end{aligned} \tag{5}$$

Recently, Hoogeboom et al. (2019) proposed a modification of the coupling layer for integer-valued variables:

$$\begin{aligned} \mathbf{y}_1 &= \mathbf{x}_1 \\ \mathbf{y}_2 &= \mathbf{x}_2 + \lfloor \text{NN}_t(x_1) \rfloor, \end{aligned} \tag{6}$$

where  $\lfloor \cdot \rfloor$  denotes the rounding operation. In order to allow applying backpropagation to the rounding operation, the straight through gradient estimator is used (Hoogeboom et al., 2019).

**Flow-based generative models** There are three major groups of generative models, namely, autoregressive models (e.g., (Van den Oord et al., 2016)), latent variable models (e.g., Variational Auto-Encoders (Kingma and Welling, 2013; Rezende et al., 2014) or GANs (Goodfellow et al., 2014)), and flow-based models (Papamakarios et al., 2019). The last approach takes advantage of the change of variables formula:

$$p(\mathbf{x}) = \pi(\mathbf{z} = f^{-1}(\mathbf{x})) |\mathbf{J}_f(\mathbf{z})|^{-1}, \tag{7}$$

where  $\pi(\cdot)$  is a known distribution (a *base* distribution, e.g., Normal distribution),  $f : \mathcal{X} \rightarrow \mathcal{X}$  is a bijective map, and  $\mathbf{J}_f(\mathbf{z})$  denotes the Jacobian matrix.

The main challenge of flow-based generative models lies in formulating invertible transformations for which the Jacobian determinant is computationally tractable. In the simplest case, we can use volume-preserving transformations that result in  $\mathbf{J}_f(\mathbf{z}) = 1$ , e.g., linear autoregressive flows (Kingma et al., 2016; Tomczak and Welling, 2017) or Householder

flows (Tomczak and Welling, 2016). However, the volume-preserving flows cannot model arbitrary distributions, therefore, non-linear transformations are preferable. In (Rezende and Mohamed, 2015; Berg et al., 2018; Hoogeboom et al., 2020) a specific form of non-linear transformations was constructed so that to take advantage of the matrix determinant lemma and its generalization to efficiently calculate the Jacobian determinant. Recently, the transformation used in (Rezende and Mohamed, 2015; Berg et al., 2018) was further generalized to arbitrary contractive residual networks (Chen et al., 2019) and contractive densenets (Perugachi-Diaz et al., 2020) with the *Russian roulette estimator* of the Jacobian determinant. Coupling layers constitute a different group of non-linear transformation that are used in flow-based models like RealNVP (Dinh et al., 2016) and GLOW (Kingma and Dhariwal, 2018).

In the case of discrete variables, e.g.,  $\mathcal{X} = \mathbb{Z}^D$ , the change of variables takes a simpler form due to the fact that there is no change of volume for probability mass functions:

$$p(\mathbf{x}) = \pi(\mathbf{z} = f^{-1}(\mathbf{x})). \tag{8}$$

To date, coupling layers with the rounding operator (see Eq. 6) are typically used. The resulting flow-based models are called Integer Discrete Flows (IDF) (Hoogeboom et al., 2019; Berg et al., 2020). In IDFs, the base distribution is a mixture of discretized logistic distributions (Salimans et al., 2017).

## 2. Our approach

In this paper, we propose a new class of invertible transformations that could be used either for real-valued variables, binary variables or integer-valued variables. We first present how various invertible transformations are special instantiations of our proposition. Further, we propose to use a different distribution than a mixture of discretized distributions that was proposed in (Chakraborty and Chakravarty, 2016). Our proposition could be used in many applications, however, here we present them in the context of the flow-based models.

### 2.1. General invertible transformations

Our main contribution of this paper is a proposition of a new class of invertible transformations that generalize many invertible transformations in reversible computing and reversible deep learning.

**Proposition 1** *Let us take  $\mathbf{x}, \mathbf{y} \in \mathcal{X}$ . The following transformation from  $\mathbf{x}$  to  $\mathbf{y}$  with  $f_i : \mathcal{X}_{1:i-1} \times \mathcal{X}_{i+1:n} \rightarrow \mathcal{X}_i$ :*

$$\begin{aligned} y_1 &= x_1 \circ f_1(\emptyset, \mathbf{x}_{2:D}) \\ y_2 &= (g_2(y_1) \triangleright x_2) \circ f_1(y_1, \mathbf{x}_{3:D}) \\ &\dots \\ y_d &= (g_d(\mathbf{y}_{1:d-1}) \triangleright x_d) \circ f_d(\mathbf{y}_{1:d-1}, \mathbf{x}_{d+1:D}) \\ &\dots \\ y_D &= (g_D(\mathbf{y}_{1:D-1}) \triangleright x_D) \circ f_D(\mathbf{y}_{1:D-1}, \emptyset) \end{aligned}$$

is invertible for given binary transformations  $\circ$  and  $\triangleright$  with inverses  $\bullet$  and  $\blacktriangleleft$ , respectively, and arbitrary functions  $g_2, \dots, g_D$  and  $f_1, \dots, f_D$ .

**Proof** In order to inverse  $\mathbf{y}$  to  $\mathbf{x}$  we start from the last element to obtain the following:

$$x_D = g_D(\mathbf{y}_{1:D-1}) \blacktriangleleft (y_D \bullet f_D(\mathbf{y}_{1:D-1}, \emptyset)).$$

Then, we can proceed with next expressions in the decreasing order (*i.e.*, from  $D - 1$  to 1) to eventually obtain:

$$\begin{aligned} x_{D-1} &= g_{D-1}(\mathbf{y}_{1:D-2}) \blacktriangleleft (y_{D-1} \bullet f_{D-1}(\mathbf{y}_{1:D-2}, x_D)) \\ &\dots \\ x_d &= g_d(\mathbf{y}_{1:d-1}) \blacktriangleleft (y_d \bullet f_d(\mathbf{y}_{1:d-1}, \mathbf{x}_{d+1:D})) \\ &\dots \\ x_2 &= g_2(y_1) \blacktriangleleft (y_2 \bullet f_2(y_1, \mathbf{x}_{3:D})) \\ x_1 &= y_1 \bullet f_1(\emptyset, \mathbf{x}_{2:D}). \end{aligned}$$

■

Next, we show that many widely known invertible transformations could be derived from the proposed general invertible transformation. First, for the space of binary variables, we present that our proposition could be used to obtain three of the most important reversible logic gates.

**Corollary 2 (Feynman gate)** *Let us consider  $\mathbf{x} \in \{0, 1\}^2$ , and  $\circ \equiv \oplus$  and  $\triangleright \equiv \oplus$  with  $\bullet \equiv \oplus$  and  $\blacktriangleleft \equiv \oplus$ , where  $\oplus$  is the XOR operation. Then, taking  $g_2 \equiv 0$ ,  $f_1(x_2) = 0$  and  $f_2(y_1) = y_1$  results in the Feynman gate:*

$$\begin{aligned} y_1 &= x_1 \\ y_2 &= x_2 \oplus x_1. \end{aligned} \tag{9}$$

**Proof** The Eq. 9 follows from the idempotency of the XOR operator. ■

**Corollary 3 (Toffoli gate)** *Let us consider  $\mathbf{x} \in \{0, 1\}^3$ , and  $\circ \equiv \oplus$  and  $\triangleright \equiv \oplus$  with  $\bullet \equiv \oplus$  and  $\blacktriangleleft \equiv \oplus$ , where  $\oplus$  is the XOR operation. Then, taking  $g_2(y_1) \equiv 0$ ,  $g_3(\mathbf{y}_{1:2}) \equiv 0$ ,  $f_1(\mathbf{x}_{2:3}) \equiv 0$ ,  $f_2(y_1, x_3) \equiv 0$  and  $f_3(\mathbf{y}_{1:2}) = y_1 \wedge y_2$  results in the Toffoli gate:*

$$y_1 = x_1 \tag{10}$$

$$y_2 = x_2 \tag{11}$$

$$y_3 = x_3 \oplus (y_1 \wedge y_2). \tag{12}$$

**Proof** The Eqs. 10 - 12 follow from the idempotency of the XOR operator. ■

**Corollary 4 (Fredkin gate)** *Let us consider  $\mathbf{x} \in \{0, 1\}^4$ , and  $\circ \equiv \oplus$  and  $\triangleright \equiv \oplus$  with  $\bullet \equiv \oplus$  and  $\blacktriangleleft \equiv \oplus$ , where  $\oplus$  is the XOR operation. Then, taking  $x_1 \equiv 0$ ,  $g_2(y_1) \equiv 0$ ,  $g_3(\mathbf{y}_{1:2}) \equiv 0$ ,  $g_4(\mathbf{y}_{1:3}) \equiv 0$ ,  $f_1(\mathbf{x}_{2:4}) = x_2 \wedge (x_3 \oplus x_4)$ ,  $f_2(y_1, \mathbf{x}_{3:4}) \equiv 0$ ,  $f_3(\mathbf{y}_{1:2}, x_4) = y_1$  and  $f_4(\mathbf{y}_{1:3}) \equiv y_1$  results in the Fredkin gate:*

$$y_1 = x_1 \oplus (x_2 \wedge (x_3 \oplus x_4)) \quad (13)$$

$$y_2 = x_2 \oplus 0 \quad (14)$$

$$y_3 = x_3 \oplus y_1 \quad (15)$$

$$y_4 = x_4 \oplus y_1 \quad (16)$$

**Remark 5 (On the Fredkin gate)** *Comparing equations 13–16 with the definition of Fredkin gate we notice that in Corollary 4 we have to introduce an additional equation to be consistent with the Proposition 1. Moreover, we introduced a dummy variable  $x_1$  that always equals 0.*

Moreover, we want to observe that our proposition generalizes invertible layers in neural networks.

**Corollary 6 (A coupling layer)** *Let us consider  $\mathbf{x} = [\mathbf{x}_1, \mathbf{x}_2]^\top$ , where  $\mathcal{X}_i = \mathbb{R}^{D_i}$ , and  $\circ \equiv +$ ,  $\triangleright \equiv \odot$  with  $\bullet \equiv -$  and  $\blacktriangleleft \equiv \oslash$ , where  $\odot$  and  $\oslash$  denote elementwise multiplication and division, respectively. Then, taking  $g_2(\mathbf{y}_1) = \exp(\text{NN}_s(\mathbf{y}_1))$ ,  $f_1(\mathbf{x}_2) = 0$  and  $f_2(\mathbf{y}_1) = \text{NN}_t(\mathbf{y}_1)$ , where  $\text{NN}_s$ ,  $\text{NN}_t$  are neural networks, results in the coupling layer (Dinh et al., 2016):*

$$\mathbf{y}_1 = \mathbf{x}_1 \quad (17)$$

$$\mathbf{y}_2 = \exp(\text{NN}_s(\mathbf{y}_1)) \odot \mathbf{x}_2 + \text{NN}_t(\mathbf{y}_1). \quad (18)$$

**Corollary 7 (A reversible residual layer)** *Let us consider  $\mathbf{x} = [\mathbf{x}_1, \mathbf{x}_2]^\top$ , where  $\mathcal{X}_i = \mathbb{R}^{D_i}$ , and  $\circ \equiv +$ ,  $\triangleright \equiv \odot$  with  $\bullet \equiv -$  and  $\blacktriangleleft \equiv \oslash$ , where  $\odot$  and  $\oslash$  denote elementwise multiplication and division, respectively. Then, taking  $g_2(\mathbf{y}_1) \equiv 1$ ,  $f_1(\mathbf{x}_2) = \text{NN}_1(\mathbf{x}_2)$  and  $f_2(\mathbf{y}_1) = \text{NN}_2(\mathbf{y}_1)$ , where  $\text{NN}$  is a neural network, results in the reversible residual layer proposed in (Gomez et al., 2017):*

$$\mathbf{y}_1 = \mathbf{x}_1 + \text{NN}_1(\mathbf{x}_2) \quad (19)$$

$$\mathbf{y}_2 = \mathbf{x}_2 + \text{NN}_2(\mathbf{y}_1). \quad (20)$$

**Remark 8 (On the reversible residual layer)** *According to Proposition 1, we can further generalize the reversible residual layer proposed in (Gomez et al., 2017) by taking  $g_2(\mathbf{y}_1) = \text{NN}_3(\mathbf{y}_1)$  that would result in the following invertible layer:*

$$\mathbf{y}_1 = \mathbf{x}_1 + \text{NN}_1(\mathbf{x}_2) \quad (21)$$

$$\mathbf{y}_2 = \text{NN}_3(\mathbf{y}_1) \odot \mathbf{x}_2 + \text{NN}_2(\mathbf{y}_1). \quad (22)$$

**Corollary 9 (A reversible differential mutation)** *Let us consider  $\mathbf{x}_1, \mathbf{x}_2, \mathbf{x}_3 \in \mathbb{R}^D$ ,  $\gamma \in \mathbb{R}_+$ , and  $\circ \equiv +$ ,  $\triangleright \equiv \odot$  with  $\bullet \equiv -$ . Then, taking  $g_2(\mathbf{y}_1) \equiv 1$ ,  $g_3(\mathbf{y}_{1:2}) \equiv 1$ ,  $f_1(\mathbf{x}_{2:3}) =$*

$\gamma(\mathbf{x}_2 - \mathbf{x}_3)$ ,  $f_2(\mathbf{y}_1, \mathbf{x}_3) = \gamma(\mathbf{x}_3 - \mathbf{y}_1)$ , and  $f_3(\mathbf{y}_{1:2}) = \gamma(\mathbf{y}_1 - \mathbf{y}_2)$ , results in the reversible differential mutation proposed in (Tomczak et al., 2020):

$$\mathbf{y}_1 = \mathbf{x}_1 + \gamma(\mathbf{x}_2 - \mathbf{x}_3) \quad (23)$$

$$\mathbf{y}_2 = \mathbf{x}_2 + \gamma(\mathbf{x}_3 - \mathbf{y}_1) \quad (24)$$

$$\mathbf{y}_3 = \mathbf{x}_3 + \gamma(\mathbf{y}_1 - \mathbf{y}_2). \quad (25)$$

## 2.2. General Invertible Transformations for Integer Discrete Flows

We propose to utilize our general invertible transformations in IDF. For this purpose, we formulate two new coupling layers that fulfill Proposition 1. Further, we propose to use a closed-form of the discretized two-parameter logistic distribution over infinite support.

### 2.2.1. A COUPLING LAYER

We formulate the following two coupling layers:

- We divide the input into four parts,  $\mathbf{x} = [\mathbf{x}_1, \mathbf{x}_2, \mathbf{x}_3, \mathbf{x}_4]$ :

$$\begin{aligned} \mathbf{y}_1 &= \mathbf{x}_1 + \lfloor \text{NN}_{t,1}(\mathbf{x}_{2:4}) \rfloor \\ \mathbf{y}_2 &= \mathbf{x}_2 + \lfloor \text{NN}_{t,2}(\mathbf{y}_1, \mathbf{x}_{3:4}) \rfloor \\ \mathbf{y}_3 &= \mathbf{x}_3 + \lfloor \text{NN}_{t,3}(\mathbf{y}_{1:2}, \mathbf{x}_4) \rfloor \\ \mathbf{y}_4 &= \mathbf{x}_4 + \lfloor \text{NN}_{t,4}(\mathbf{y}_{1:3}) \rfloor \end{aligned} \quad (26)$$

- We divide the input into eight parts,  $\mathbf{x} = [\mathbf{x}_1, \dots, \mathbf{x}_8]$ . Then, we formulate the coupling layer analogously to (26).

### 2.2.2. BASE DISTRIBUTION OVER INTEGERS WITH INFINITE SUPPORT

Chakraborty and Chakravarty (2016) proposed a new distribution over integers with infinite support that is the discretized two-parameter logistic distribution. The probability mass function (pmf) takes the following closed-form (Chakraborty and Chakravarty, 2016):

$$P(Y = y) = \frac{(1-p)p^{y-\mu}}{(1+p^{y-\mu})(1+p^{y-\mu+1})}, \quad (27)$$

where  $y \in \mathbb{Z}$ ,  $p \in (0, 1)$ ,  $\mu \in \mathbb{R}$ , and the negative logarithm of the pmf is as follows:

$$-\ln P(Y = y) = -\ln(1-p) - (y-\mu) \ln p + \ln(1+p^{y-\mu}) + \ln(1+p^{y-\mu+1}). \quad (28)$$

We propose to utilize this closed-form pmf of the discretized distribution because it could be used explicitly to integer values instead of normalizing integer values and applying the difference of the cumulative distribution function of the logistic distribution as in (Salimans et al., 2017). Moreover, as suggested by Berg et al. (2020), truncating integers to values of pixels, i.e., from 0 to 255, drastically limits the flexibility of the IDF.

## 3. Experiments

**Data** In the experiment, we use a toy dataset of handwritten digits available in Scikit-learn<sup>1</sup> that consists of 1,797 images. Each image consists of 64 pixels (8px×8px).

1. <https://scikit-learn.org/stable/datasets/index.html#digits-dataset>

**Models** In the experiment, we compare the following models:

- RealNVP with uniform dequantization and the standard Gaussian base distribution (REALNVP).
- IDF with the coupling layer in (6) (REALNVP).
- IDF with the coupling layer in (26) (IDF4).
- IDF with the coupling layer for eight parts (IDF8).

In all models, we used the order permutation (i.e., a matrix with ones on the anti-diagonal and zeros elsewhere) after each coupling layer.

In order to keep a similar number of weights, we used 16 flows for IDF, 8 flows for REALNVP, 4 flows for IDF4, and 2 flows for IDF8. All models have roughly 1.32M weights. For IDF, IDF4, and IDF8 we utilized the following neural networks for transitions ( $\text{NN}_t$ ):

$$\text{Linear}(D_{in}, 256) \rightarrow \text{LeakyReLU} \rightarrow \text{Linear}(D_{in}, 256) \rightarrow \text{LeakyReLU} \rightarrow \text{Linear}(256, D_{out})$$

and for REALNVP, we additionally used the following neural networks for scaling ( $\text{NN}_s$ ):

$$\begin{aligned} &\text{Linear}(D_{in}, 256) \rightarrow \text{LeakyReLU} \rightarrow \text{Linear}(D_{in}, 256) \rightarrow \text{LeakyReLU} \rightarrow \\ &\quad \rightarrow \text{Linear}(256, D_{out}) \rightarrow \text{Tanh} \end{aligned}$$

**Training & Evaluation** We compare the models using the negative-log likelihood (nll), see Eq. 28. We train each model using 1,000 images, and the mini-batch equals 64. Moreover, we take 350 images for validation and 447 for testing. Each model is trained 5 times. During training, we use the early stopping with the patience equal 20 epochs, and the best performing model on the validation set is later evaluated on the test set. The Adam optimizer with the learning rate equal 0.001 was used.

**Code** The experiments could be reproduced by running the code available at: [https://github.com/jmtomczak/git\\_flow](https://github.com/jmtomczak/git_flow)

**Results** In Figure 1, we present aggregated results for the four models. In Table 1 the average nlls with standard deviations are gathered. Moreover, in Figure 2, examples of unconditional samples are presented, together with a real sample.

Table 1: The test negative log-likelihoods (average  $\pm$  standard deviation).

Model	IDF	IDF4	IDF8	REALNVP
nll $\downarrow$	141.99 $\pm$ 0.40	137.07 $\pm$ 0.32	<b>133.42</b> $\pm$ 0.48	147.84 $\pm$ 3.54

First, we notice that IDF performs better than REALNVP. In this paper, we use fully-connected neural networks and small toy data. Nevertheless, it is interesting to see that IDF could perform better than a widely used continuous flow-based model with dequantization.

Second, we observe that our proposition of invertible transformations results in the improved nll. The proposed coupling layer with 8 partitions performed the best in terms of nll, and the coupling layer with 4 partitions also outperformed IDF and REALNVP.

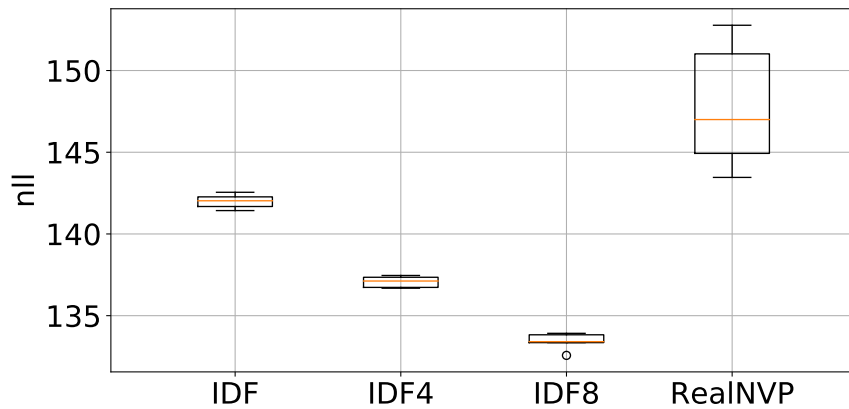


Figure 1: The aggregated results for the four models on the test set.

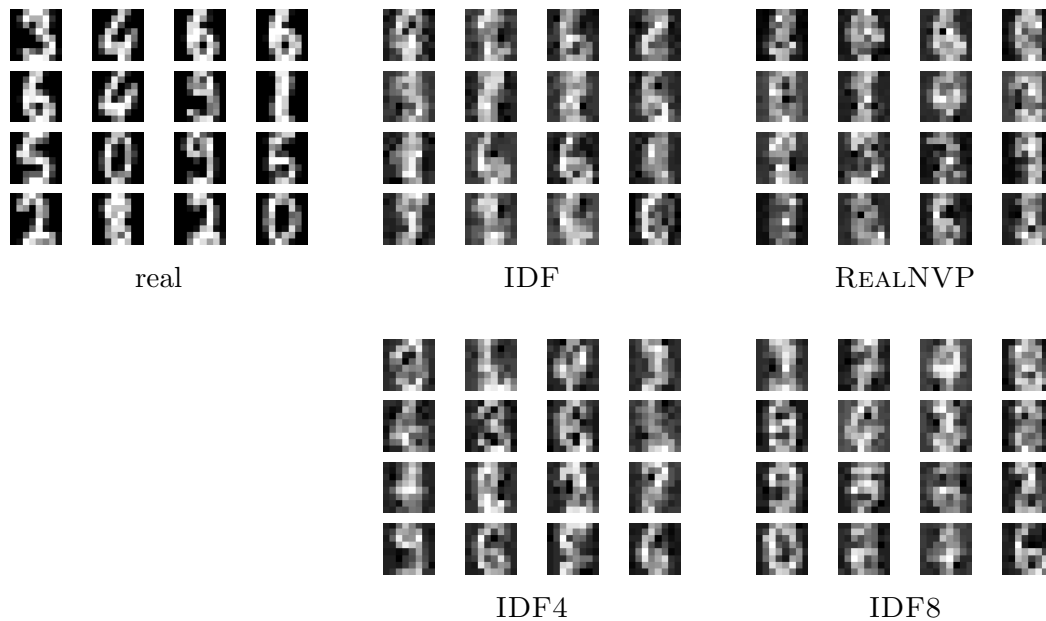


Figure 2: Unconditional samples from the four models.

We want to highlight that all models have almost identical numbers of weights, thus, these results are not caused by taking larger neural networks.

The samples presented in Figure 2 are rather hard to analyze due to their small size (8px×8px). Nevertheless, we notice that all IDFs generated crisper images than REALNVP. Moreover, it seems that IDF4 and IDF8 seem to produce digits of higher visual quality. However, we do not claim that this experiment is conclusive, but it is definitely encouraging.

#### 4. Conclusion

In this paper, we proposed a new class of invertible transformations. We showed that many well-known invertible transformations could be derived from our proposition. Moreover, we proposed two coupling layers and presented how they could be utilized in flow-based models for integer values (Integer Discrete Flows). Our preliminary experiments on the digits data indicate that the new coupling layers result in better negative log-likelihood values than for IDF and REALNVP. These results are promising and will be pursued in the future on more challenging datasets.

#### References

- Charles H Bennett. Notes on landauer’s principle, reversible computation, and maxwell’s demon. *Studies In History and Philosophy of Science Part B: Studies In History and Philosophy of Modern Physics*, 34(3):501–510, 2003.
- Rianne van den Berg, Leonard Hasenclever, Jakub M Tomczak, and Max Welling. Sylvester normalizing flows for variational inference. *UAI*, 2018.
- Rianne van den Berg, Alexey A Gritsenko, Mostafa Dehghani, Casper Kaae Sønderby, and Tim Salimans. Idf++: Analyzing and improving integer discrete flows for lossless compression. *arXiv preprint arXiv:2006.12459*, 2020.
- Subrata Chakraborty and Dhruvajyoti Chakravarty. A new discrete probability distribution with integer support on  $(-\infty, \infty)$ . *Communications in Statistics-Theory and Methods*, 45(2):492–505, 2016.
- Bo Chang, Lili Meng, Eldad Haber, Lars Ruthotto, David Begert, and Elliot Holtham. Reversible architectures for arbitrarily deep residual neural networks. In *AAAI*, 2018.
- Ricky TQ Chen, Jens Behrmann, David K Duvenaud, and Jörn-Henrik Jacobsen. Residual flows for invertible generative modeling. In *Advances in Neural Information Processing Systems*, pages 9916–9926, 2019.
- Laurent Dinh, Jascha Sohl-Dickstein, and Samy Bengio. Density estimation using real nvp. *arXiv preprint arXiv:1605.08803*, 2016.
- Richard P Feynman. Quantum mechanical computers. *Foundations of physics*, 16(6):507–531, 1986.
- Edward Fredkin and Tommaso Toffoli. Conservative logic. *International Journal of theoretical physics*, 21(3-4):219–253, 1982.

- Aidan N Gomez, Mengye Ren, Raquel Urtasun, and Roger B Grosse. The reversible residual network: Backpropagation without storing activations. In *NIPS*, pages 2214–2224, 2017.
- Ian Goodfellow, Jean Pouget-Abadie, Mehdi Mirza, Bing Xu, David Warde-Farley, Sherjil Ozair, Aaron Courville, and Yoshua Bengio. Generative adversarial nets. In *NIPS*, pages 2672–2680, 2014.
- Emiel Hoogeboom, Jorn Peters, Rianne van den Berg, and Max Welling. Integer discrete flows and lossless compression. In *Advances in Neural Information Processing Systems*, pages 12134–12144, 2019.
- Emiel Hoogeboom, Victor Garcia Satorras, Jakub M Tomczak, and Max Welling. The convolution exponential and generalized sylvester flows. *NeurIPS*, 2020.
- Diederik P Kingma and Max Welling. Auto-encoding variational bayes. *arXiv preprint arXiv:1312.6114*, 2013.
- Durk P Kingma and Prafulla Dhariwal. Glow: Generative flow with invertible 1x1 convolutions. In *NeurIPS*, pages 10215–10224, 2018.
- Durk P Kingma, Tim Salimans, Rafal Jozefowicz, Xi Chen, Ilya Sutskever, and Max Welling. Improved variational inference with inverse autoregressive flow. In *NIPS*, pages 4743–4751, 2016.
- Matthew MacKay, Paul Vicol, Jimmy Ba, and Roger B Grosse. Reversible recurrent neural networks. In *NeurIPS*, pages 9029–9040, 2018.
- George Papamakarios, Eric Nalisnick, Danilo Jimenez Rezende, Shakir Mohamed, and Balaji Lakshminarayanan. Normalizing flows for probabilistic modeling and inference. *arXiv preprint arXiv:1912.02762*, 2019.
- Yura Perugachi-Diaz, Jakub M Tomczak, and Sandjai Bhulai. i-densenets. *arXiv preprint arXiv:2010.02125*, 2020.
- Danilo Rezende and Shakir Mohamed. Variational inference with normalizing flows. In *ICML*, pages 1530–1538, 2015.
- Danilo Jimenez Rezende, Shakir Mohamed, and Daan Wierstra. Stochastic backpropagation and approximate inference in deep generative models. In *ICML*, 2014.
- Tim Salimans, Andrej Karpathy, Xi Chen, and Diederik P Kingma. Pixelcnn++: Improving the pixelcnn with discretized logistic mixture likelihood and other modifications. *arXiv preprint arXiv:1701.05517*, 2017.
- Tommaso Toffoli. Reversible computing. In *International Colloquium on Automata, Languages, and Programming*, pages 632–644. Springer, 1980.
- Jakub M Tomczak and Max Welling. Improving variational auto-encoders using householder flow. *arXiv preprint arXiv:1611.09630*, 2016.

Jakub M Tomczak and Max Welling. Improving variational auto-encoders using convex combination linear inverse autoregressive flow. *arXiv preprint arXiv:1706.02326*, 2017.

Jakub M Tomczak, Ewelina Weglarz-Tomczak, and Agoston E Eiben. Differential evolution with reversible linear transformations. *arXiv preprint arXiv:2002.02869*, 2020.

Aaron Van den Oord, Nal Kalchbrenner, Lasse Espeholt, Oriol Vinyals, Alex Graves, et al. Conditional image generation with pixelcnn decoders. In *NIPS*, pages 4790–4798, 2016.

## Appendix A. Properties of XOR and AND

Main properties of the XOR operator:

- $x \oplus 0 = x$ ,
- No idempotency (self-inverse):  $x \oplus x = 0$ ,
- Comutative:  $x \oplus y = y \oplus x$ ,
- Associativity:  $x \oplus (y \oplus z) = (x \oplus y) \oplus z$ .

Main properties of the logic AND operator:

- $x \wedge 0 = 0$ ,
- $x \wedge 1 = x$ ,
- Idempotency:  $x \wedge x = x$ ,
- Comutative:  $x \wedge y = y \wedge x$ ,
- Associativity:  $x \wedge (y \wedge z) = (x \wedge y) \wedge z$ ,
- Complementation:  $x \wedge \neg x = 0$ .